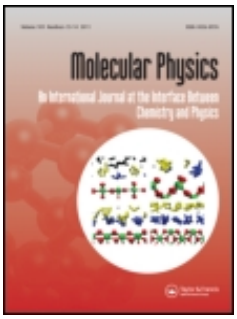

Taylor & Francis
Taylor & Francis Group

Molecular Physics

An International Journal at the Interface Between Chemistry and Physics

ISSN: 0026-8976 (Print) 1362-3028 (Online) Journal homepage: https://www.tandfonline.com/loi/tmph20

Molecular dynamics study of water in contact with the TiO_2 rutile-110, 100, 101, 001 and anatase-101, 001 surface

Ritwik S. Kavathekar , Pratibha Dev , Niall J. English & J.M.D. MacElroy

To cite this article: Ritwik S. Kavathekar , Pratibha Dev , Niall J. English & J.M.D. MacElroy (2011) Molecular dynamics study of water in contact with the TiO_2 rutile-110, 100, 101, 001 and anatase-101, 001 surface, Molecular Physics, 109:13, 1649-1656, DOI: 10.1080/00268976.2011.582051

To link to this article: https://doi.org/10.1080/00268976.2011.582051

Molecular Physics
Vol. 109, No. 13, 10 July 2011, 1649–1656

Taylor & Francis
Taylor & Francis Group

RESEARCH ARTICLE

Molecular dynamics study of water in contact with the TiO_2 rutile-110, 100, 101, 001 and anatase-101, 001 surface

Ritwik S. Kavathekar, Pratibha Dev, Niall J. English* and J.M.D. MacElroy

The SFI Strategic Research Cluster in Solar Energy Conversion and the Centre for Synthesis and Chemical Biology, School of Chemical and Bioprocess Engineering, University College Dublin, Belfield, Dublin 4, Ireland

(*Received 15 March 2011; final version received 12 April 2011*)

We have carried out classical molecular dynamics of various surfaces of TiO_2 with its interface with water. We report the geometrical features of the first and second monolayers of water using a Matsui Akaogi (MA) force field for the TiO_2 surface and a flexible single point charge model for the water molecules. We show that the MA force field can be applied to surfaces other than rutile (110). It was found that water OH bond lengths, H–O–H bond angles and dipole moments do not vary due to the nature of the surface. However, their orientation within the first and second monolayers suggest that planar rutile (001) and anatase (001) surfaces may play an important role in not hindering removal of the products formed on these surfaces. Also, we discuss the effect of surface termination in order to explain the layering of water molecules throughout the simulation box.

Keywords: molecular dynamics; TiO_2 surface; oxide–water interface; rutile; anatase

1. Introduction

Titanium dioxide (TiO_2) surfaces have been of most interest for the photochemical degradation of organic compounds such as bactericides and hydrophobic coatings [1], and show considerable potential in the field of solar energy conversion by mediation of the photocatalytic splitting of water, as demonstrated by the Fujishma–Honda reaction [2]. This reaction is a four-hole mechanism [3], producing O_2/H_2 gas, and takes place in the presence of solar radiation and in the absence of external bias. Electron–hole pairs are generated in the bulk and migrate towards the surface where the hole reacts with water. Although several materials have been used as photocatalysts for H_2/O_2 production, such as nanoribbons of CdSe–MoS_2 [4], core (GaN:ZnO)-shell (Cr_2O_3) [5], oxynitrides [6], BiVO on reduced graphene [7], phosphate-based Co^{2+} catalysts [8], algae [9], and, more recently, Fe_2O_3 [10], TiO_2 remains a strong contender due to its stability, cost-effectiveness and non-toxicity. It is clear that the structure of the TiO_2–water interface plays a great role in enhancing the efficiency of photolysis. Rutile is the most abundant polymorph of TiO_2 and the (110) face is the most stable surface. The pristine (110) surface is inert, but water splitting takes place at defect sites [11] created by oxygen vacancies, and much experimental [12] and theoretical [13–16] scrutiny has consequently been directed thereto. Water molecules may undergo dissociative or molecular adsorption, or both [1]. One of the early calculations proposing mixed water adsorption modes was by Lindan *et al.* [17], based on a first-principles approach. Quasi-elastic neutron scattering (QENS) studies along with molecular dynamics (MD) [18] have demonstrated that water molecules form hydrogen-bonded second and third layers above the (110) surface. Back-scattering neutron spectroscopy reports [19], supported by MD, show that, on average, participation of water molecules in four hydrogen bonds is needed for slow dynamical ('Arrhenius-type') behavior, while that fast dynamics ('non-Arrhenius-type') is possible if less than three hydrogen bonds are present, depending on the level of hydration. Most of the reported work [15,16,20] on water adsorption on rutile (110) deals with adsorption isotherm prediction, surface charging effects using the multisite complexation model (MUSIC) and correlating behavior with pH titration employing both classical and quantum chemical approaches. Density functional theory using plane-augmented wave potentials have been used [15] to model photooxidation of water with detailed energetic analysis. Also, some solvation studies of TiO_2 surfaces using reaction fields and conductor-like screening models for real solvents (COSMO-RS) have been

*Corresponding author. Email: niall.english@ucd.ie

ISSN 0026–8976 print/ISSN 1362–3028 online

DOI: 10.1080/00268976.2011.582051
http://www.informaworld.com

reported [16] for predicting proton affinity for the surface. Another important rutile surface is (100), which, along with (110), contributes to the reaction mechanism of photocatalytic water-splitting. *Ab initio* simulations based on Car–Parrinello Molecular Dynamics (CPMD) on perfect and defect rutile (110) and rutile (100) surfaces [21] resulted only in weakly stabilized H_2O molecule on the pristine surface. But OH dissociation was observed on the defective (creation of an oxygen vacancy) rutile (100) surface and not on the perfect and defect rutile (110) surfaces, as postulated. Rutile (101) and (100) facets contribute to about 20% each of the total crystal surface, with rutile (100), and thus these constitute particularly important surfaces for water absorption. Although most studies have been performed using quantum methods, classical dynamics remains an important tool for studying larger picosecond time scale phenomena with macroscopically observed properties.

2. Simulation methodology

Anhydrous rutile (110), (100), (101), (001) and anatase (101), (001) surface geometries were realized in slab configurations in the x–y plane and water molecules added in the z-direction for at least 50 Å distance. The respective molecular compositions and structural details for relaxed water–titania interfaces are specified in Table 1. Classical molecular dynamics was performed in the NVT ensemble at 300 K using DL_POLY [22] in conjunction with a Nosé–Hoover thermostat, the three-dimensional Ewald summation for long-range electrostatic interactions with a relative precision within 10^{-5} and the Velocity–Verlet scheme with a time step of 1 fs. All production simulations were run for 1 ns after 200 ps of equilibration. All simulations were periodic in three dimensions. We used the force field as reported by Bandura *et al.* [14] and Predota *et al.* [20] for all surfaces and the water model and cross-interaction parameters are summarized in Table 2. For the crystal, the Matsui and Akaogi (MA) [23] parameters were used, while water was represented by a Lennard–Jones potential with a harmonic H_w–O_w–H_w angle potential and a Morse-stretch O_w–H_w bond potential. Water bond angles and bond lengths were not constrained and thus a flexible SPC model was used. Using a classical Morse stretching potential enables one to follow bond-length changes during the course of the simulation. This, however, is a non-dissociative model and is thus unable to reproduce water splitting or OH dissociation. In the present work, we are interested primarily in the orientation and detection of any strain on the water molecules within the monolayers. The entire TiO_2 block was mobile for all surfaces throughout the simulation.

Table 1. Details of the geometries used.

Phase (surface)	X, Y, Z (Å)	System size
Rutile (110)	26.26, 45.47, 69.490	$(TiO_2)_{630}(H_2O)_{2000}$
Rutile (100)	22.97, 26.63, 70.00	$(TiO_2)_{405}(H_2O)_{950}$
Rutile (101)	27.33, 27.56, 113.47	$(TiO_2)_{300}(H_2O)_{2468}$
Rutile (001)	22.97, 22.97, 124.00	$(TiO_2)_{400}(H_2O)_{1720}$
Anatase (101)	71.46, 26.43, 72.680	$(TiO_2)_{1176}(H_2O)_{3162}$
Anatase (001)	33.98, 33.98, 124.00	$(TiO_2)_{648}(H_2O)_{3900}$

Table 2. Force field parameters.

Buckingham potential for TiO_2 and water oxygen: $A_{ij}\exp(-r_{ij}/\rho_{ij}) - C_{ij}/r_{ij}^6$			
i–j	A_{ij} (kcal mol^{-1})	ρ_{ij} (Å)	C_{ij} (kcal mol^{-1} Å^6)
Ti–O	391,049.1	0.194	290.331
Ti–Ti	717,647.4	0.154	121.067
O–O	271,716.3	0.234	696.888
Ti–O_w	28,593.0	0.265	148.000
Lennard–Jones potential for water: $(q_iq_j/r_{ij}) + \varepsilon_{ij}[(\sigma_{ij}/r_{ij})^{12} - (\sigma_{ij}/r_{ij})^6]$			
i–j	ε_{ij} (kcal mol^{-1})	σ_{ij} (Å)	
O_w–O_w	0.15539	3.5532	
Morse bond potential for water: $A_{ij}[1 - \exp(-k_{ij}(r_{ij} - r_{ij}^0)]^2 - A_{ij}$			
i–j	A_{ij} (kcal mol^{-1})	k_{ij} (Å^{-1})	r_{ij}^0 (Å)
O_w–H_w	101.905	2.347	1.00
Harmonic angle bending potential for water: $k/2 \times (\theta - \theta_0)$			
i–j–k	θ_0 (deg)	k (kcal mol^{-1} rad^{-2})	
H–O–H	109.47	103.045	
Atomic charges: q(Ti) = 2.196e, q(O) = −1.098e, q(O_w) = −0.82e, q(H_w) = 0.41e; O_w, H_w = water oxygen and hydrogen atoms			

Bulk rutile is defined by lattice vectors of length $a_0 = b_0 = 4.593$ Å, $c_0 = 2.959$ Å with symmetry group P42/MNM. Bulk anatase has lattice vectors $a_0 = b_0 = 3.776$ Å and $c_0 = 9.486$ Å and symmetry group I41/AMD. All surfaces were constructed by cleaving super cells made from bulk crystals. The rutile (110) surface (Figure 1(a)) is the most thermodynamically stable and constitutes a major part of the bulk TiO_2 surface. The (110) surface was reconstructed for charge auto-compensation [1]. The rutile (110) oxygen-terminated surface is non-polar [24] and hence a dipole-free surface was ensured. The rutile (110) surface consists of bridging oxygen atoms bonded to six-coordinated titania (Ti_{6c}) and a three-coordinated oxygen (O_{3c}) bonded to Ti_{5c} and Ti_{6c} atoms. These Ti_{5c} surface atoms were used as the plane against which height measurements of water oxygen (O_w) atoms were made. Surface termination produces coordinatively unsaturated sites (CUS), which differ in charge from the bulk. Although surface-modified charges are available [14] for the rutile (110) surface, they have not been specified for other surfaces, to the best of the authors' knowledge. The rutile (100) surface (Figure 1(b)) constitutes about 20% of the bulk rutile and has a ridge pattern created by two-coordinated bridging oxygen atoms connected to Ti_{5c}. The rutile (100) surface is similar to that of rutile (110), except that the bridging plane Ti_{5c}–O_b–Ti_{5c} is inclined at an angle, rather than perpendicular as in (110). The rutile (101) plane (Figure 1(c)) is similar to that of rutile (100) and also composes 20% of naturally occurring rutile. It is also composed of Ti_{5c} and O_{2c} structures, but the Ti_{5c} bond length differs to the O_{2c}, creating two different types of O_{2c}. Also, the rutile (101) plane is tilted with respect to the z-direction (chosen as the standard orientation for solvation, as mentioned previously), and was rotated for alignment *vis-à-vis* the z-direction. The rutile (001) surface (Figure 1(d)) forms a lesser part of naturally occurring rutile, and although only a few experiments have been performed on this surface, it was considered in this study for the sake of completeness and comparison. The rutile (001) surface has four-coordinated Ti atoms (Ti_{4c}) bonded to O_{2c} atoms, along with alternating Ti_{6c} atoms bonded to O_{2c} atoms, giving it a corrugated, ridge-like structure. This surface is comparatively more acidic due to large-coordinate unsaturation (CUS) of Ti_{4c} atoms. It is also unstable and hence difficult to study experimentally due to spontaneous reconstruction of the surface.

Anatase is the more photoactive polymorph than rutile and is also reported [25] to be an efficient candidate for photoelectrolysis of water. It is also used in other solar-energy-based applications such as dye-sensitized solar cells, and therefore the water–anatase interface constitutes an important system for comparative studies *vis-à-vis* rutile. The anatase (101) surface (Figure 2(a)) exhibits a terrace-like structure formed by

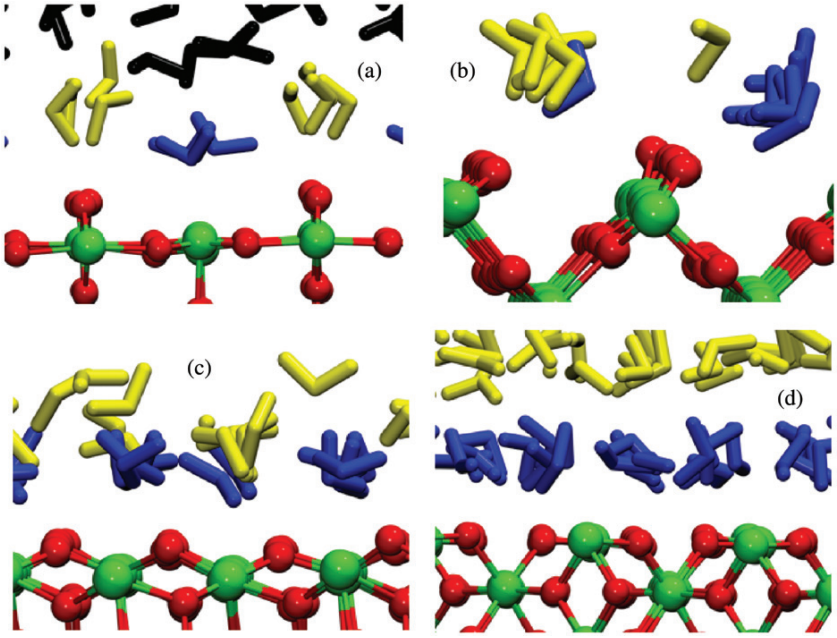

Figure 1. Representative configurations of various rutile–water interfaces: (a) (110), (b) (100), (c) (101) and (d) (001).

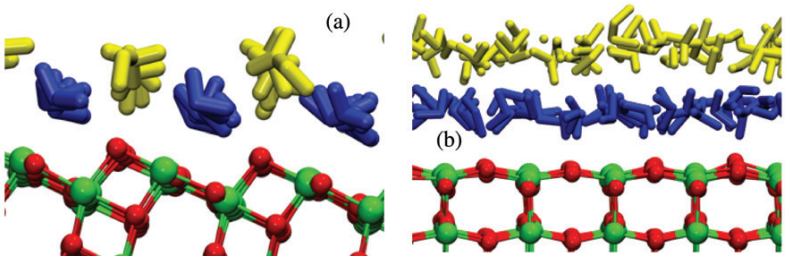

Figure 2. Representative configurations of various anatase–water interfaces: (a) (101) and (b) (001).

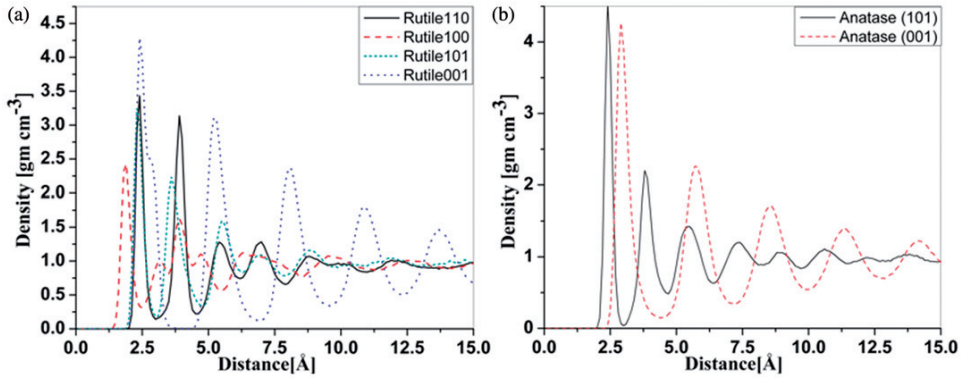

Figure 3. Absolute density ($g\,cm^{-3}$) of water above various planes of (a) rutile and (b) anatase. The plane formed by the first surface titanium atoms was used for projection of the vectors (see text for details).

fully coordinated Ti_{6c} atoms bonded to O_{3c} atoms and under-coordinated Ti_{5c} with O_{2c}. The surface is tilted at an angle with respect to the [101] direction and was rotated to align with the *z*-axis, i.e. [001]. Although the pristine anatase (101) surface is inert to photolysis, some reports have indicated dissociative adsorption onto anatase (001) surfaces [25]. The anatase (001) face is not stable, and various instances of this have been reported [1]. Anatase (001) (Figure 2(b)) has a flat plane connected by alternating rows of Ti_{5c} and O_{2c} atoms in a three- and two-fold manner, respectively. Surfaces can be made non-polar [24] by varying the surface termination. This surface dipole effect was manifested in our simulations wherein water was found to layer on top of such dipole 'non-free' surfaces.

3. Results and discussion

The density distributions, based on the distances of the water oxygen (O_w) atoms from the crystal plane, are depicted in Figure 3. The density of water was calculated as the mass of the number of water molecules per 0.1 Å volume increment away from the surface (counting a molecule present if its O_w is in each grid element), i.e. along the direction of heterogeneity (the *z*-direction). This density profile was used as a guide to sample the respective properties in consecutive layers. Figure 3(a) shows that the order of distance to the rutile plane is (100) < (101) < (110) = (001). The plane used for calculation of the distance to O_w atoms was taken to be the first Ti plane found on the surface. The distance for rutile (100) is found to be 1.9 Å, due to the (electrostatic) attraction of Ti_{5c} atoms below the O_{2c} to the water oxygen atoms. This is similar to the (101) case, for which the first exposed plane is formed by O_{2c} atoms, but the Ti_{5c} atoms are bonded to the O_{2c} atoms in the same plane, and hence the water oxygen atoms are at approximately 2.3 Å distance due to O_{2c}–O_w repulsion compensated by Ti_{5c}–O_{2c} attraction. The (110) surface plane was taken to be that formed by Ti_{5c} rather than the bridging oxygen atoms. Water molecules occupy the spaces in between the Ti_{5c} (probably owing to the tetrahedral water geometry formed by two hydrogen atoms and two lone pairs), rather than on top of it. For the (001) surface, alternated with O_{2c} and Ti_{4c} sites, the H_w are therefore tilted towards the O_{2c} atoms, creating a tilt angle and

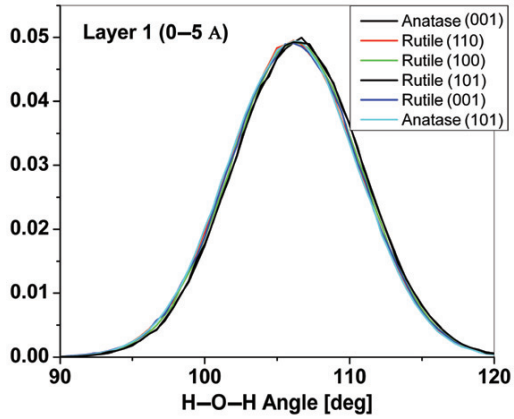

Figure 4. Probability distribution of the water H_w–O_w–H_w angle in the adsorbed monolayer in contact with each surface.

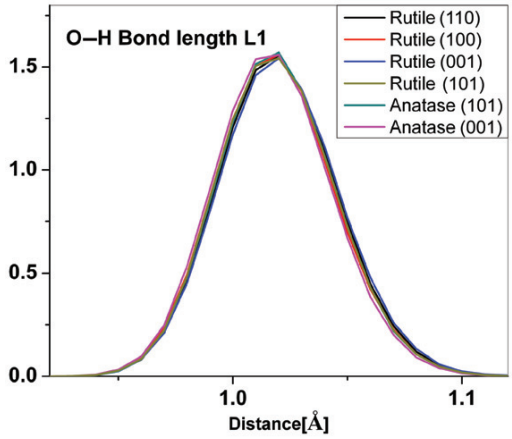

Figure 5. Distribution of the water O_w–H_w bond length in the adsorbed monolayer in contact with each surface.

'pulling' the water molecule inwards. For anatase surfaces, the order of distance to the plane is in the order (101) < (001). The (101) ridged, terrace-like structure permits the water molecules to remain in between the O_{2c} atoms, binding more weakly to the Ti_{5c} surface atoms, whilst remaining hydrogen-bonded to O_{2c} atoms. The anatase (001), planar surface creates a flat monolayer, at a distance of 2.5 Å. Previous calculations using similar force fields have been reported [20] (see also references therein). However, these simulations [20] were performed on stationary surfaces derived from quantum simulations with a rigid SPC water model, 3D Ewald sum with correction for 2D periodic geometry electrostatics at 298.15 K temperature. They reported a *z*-axis density profile distance for water oxygens at 2.2 Å for the neutral rutile (110) surface. CPMD simulations [26] for anatase (101) and (001) surfaces showed dissociative adsorption of water molecules on anatase (001). The Ti_{5c}–O_w (dissociated water) distance was reported to be 1.84 Å and Ti_{5c}–O_w (molecular water) was observed at 2.14. They observed no dissociation on pristine anatase (101).

In order to investigate intramolecular strain in the water molecules at the interface we calculated, as depicted in Figures 4 and 5, respectively, the probability distributions of water (H_w–O_w–H_w) angles and O_w–H_w bond lengths in the adsorbed monolayer (evident from the density profiles of Figure 3, and labeled 'L1'). However, no significant shifts were found for interfacial, adsorbed water molecules relative to bulk water molecules. The average bond angle in the adsorbed layer was 106.11° compared with 107.22° in the bulk for the rutile (101) case, while for the anatase (101) case, the adsorbed layer's angle was 105.55°

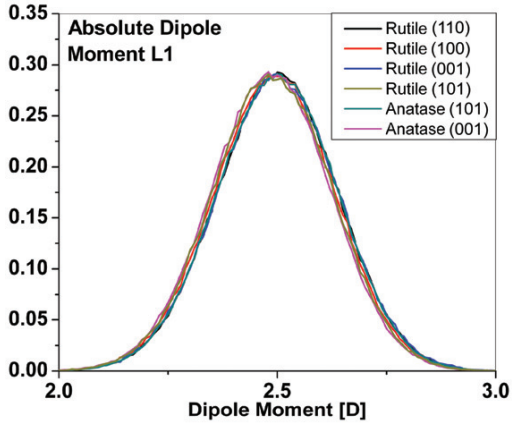

Figure 6. Distribution of the water absolute dipole moment in the adsorbed monolayer in contact with each surface.

compared with 106.66° in the bulk liquid. Also, the O_w–H_w bond length showed no significant deviation between L1 and the bulk, with the average bond length (Figure 5) being 1.02 Å. This geometry is close to the values of 108.5° and 0.98 Å for the water angle and bond length, respectively, reported [27] with plane-wave-based *ab inito* DFT using the GGA functional on the rutile (110) surface, which were modeled for STM experiments.

We calculated the distribution profiles for the molecular dipole moment of water (Figure 6) in L1 and found the average value to be at 2.4 D, without significant deviation from the other layers, which is consistent with the value of condensed water [28] at all

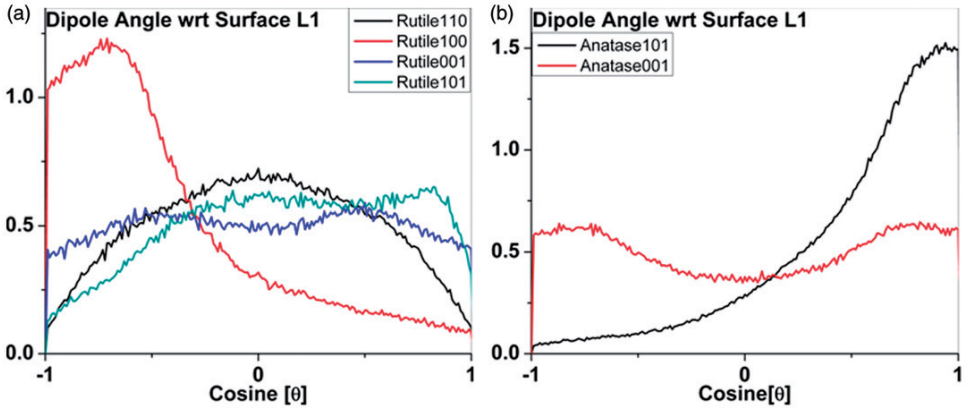

Figure 7. Distribution of the cosine of the angle of the monolayer's water molecules' dipole vectors with respect to the plane of the crystal surface, θ, for various faces of (a) rutile and (b) anatase. A cosine of zero indicates dipole alignment normal to the face, while ± 1 indicates parallel dipole alignment, oriented parallel, or along the surface.

interfaces. This is consistent with the water bond angles and bond lengths in all simulations. Figure 7 shows the angle made by a vector on the titania surface and the molecular dipole moment vector of water. It can be seen that, at the rutile (110)–water interface, the dipole vector points downwards making a 90° angle with the surface. However, for the rutile (001) and anatase (001) surfaces, the vectors are pointed along the surface on either side. Water dipole vectors at the rutile (100) surface are oriented in one direction along the surface, while, for rutile (101), the water dipole vectors point towards and along the surface. Sampling between the regions within 5 Å of the interface involves at least two water monolayers, as seen in Figure 3. Calculating water dipole moment vectors at these monolayer distances resolves the orientation more clearly, as shown in Figure 8. Rutile (110) (Figure 8(a)) distinguishes between the first and second monolayer (ML) dipole vector orientations of water at distance of 2.4 and 3.9 Å, respectively. The first ML water molecules are oriented perpendicular to the surface, as depicted in Figure 1(a) (black/dark shade), and the second ML (yellow/light shade) dipole moment vectors point along either side of the surface. Water molecules in both monolayers are stabilized by hydrogen bonding with bridging oxygens of rutile (110). The rutile (100) face has a slanting, roof-like structure with bridging oxygens at the edges, hence their angles are off to one side along the surface (Figure 1(b)), with the first ML and second ML waters appearing at distances of 1.9 and 3.1 Å, respectively. The first ML and second ML for rutile (101) appear at 2.3 and 3.6 Å with a spread of angles in the second ML and a partial orientation in the first ML, owing to the serrated nature of the surface. The second ML waters have H_w atoms bonding with bridging oxygens with O_w pointing opposite to the z-direction and the first ML waters spread in a perpendicular direction with O_w pointing towards Ti_{5c}. The rutile (001) surface is planar, where Ti_{4c} atoms are sandwiched between O_{2c} competing with H-bonding with water molecules, giving them an angular orientation with O_w pointing towards Ti_{4c}. This pushes the second ML away to 5.2 Å from the first ML at 2.4 Å. A small shoulder at 2.8 Å in the density distribution of rutile (001) (Figure 3(a)) indicates a second orientation within the first ML with H_w pointing towards O_{2c} atoms. The anatase (101) surface is similar to rutile (100) except that Ti and O layers alternate in the x-direction, hence their angles are similar, i.e. along the surfaces. The anatase (101) first ML and second ML occur at 2.4 and 3.8 Å, respectively. Anatase (001), like rutile (001), is a planar surface, but much flatter without any 'cavities', thus creating denser and uniform first and second monolayers. The anatase (001) first and second ML are at 2.9 and 5.7 Å, respectively.

4. Conclusions

We have performed classical molecular dynamics of rutile (110), (101), (001), (001) and anatase (101), (001) faces for polymorphs of TiO_2 in contact with water, using a flexible Morse potential for water and the Matsui–Akaogi potential for the crystal, where the entire crystal block is mobile and not fixed/constrained. Newer force field models employing polarization effects, as recently suggested by Han *et al.* [29],

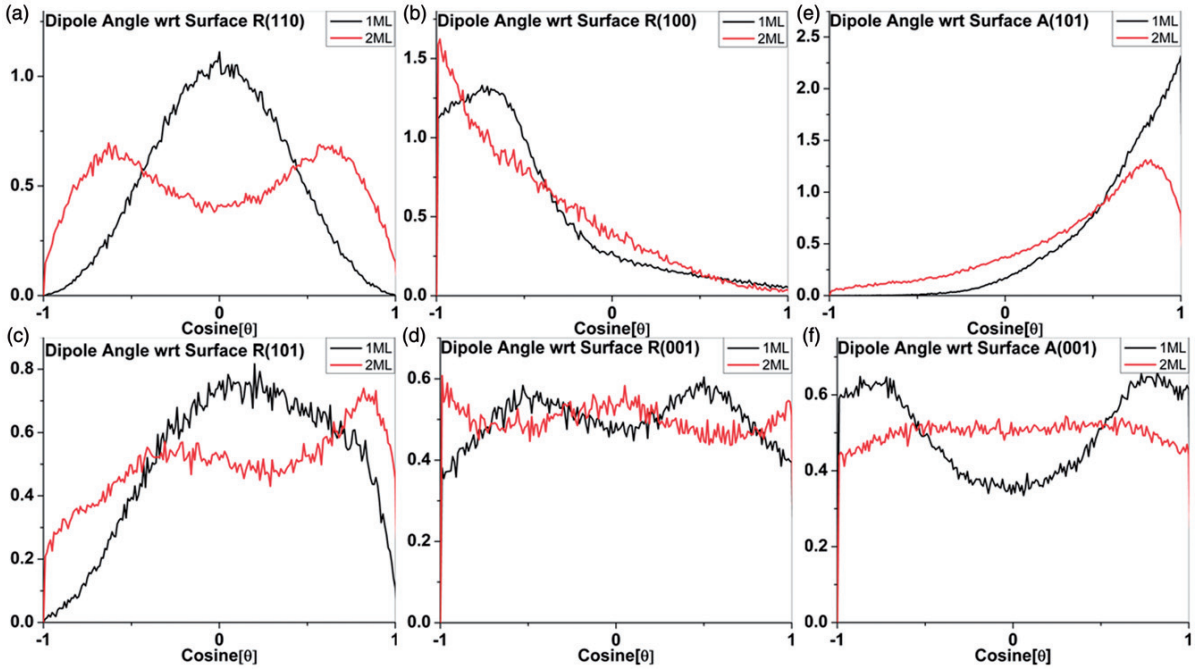

Figure 8. Distribution of the cosine of the angle of the first two layers of the water molecules' dipole vectors with respect to the plane of the crystal surface, θ, for various faces: (a) rutile (110), (b) rutile (100), (c) rutile (101), (d) rutile (001), (e) anatase (101) and (f) anatase (001). A cosine of zero indicates dipole alignment normal to the face, while ± 1 indicates parallel dipole alignment, oriented parallel, or along the surface.

would perhaps be a good approach for modeling the flexible lattice; in this case [29], phonon dispersion curves were fitted with *ab initio* density functional theory (LDA) to the classical force field model. The orientation of the water molecules depends heavily on the surface terminations of either side of the solid surfaces. Analysis of the distribution profiles of O_w–H_w bond lengths and H_w–O_w–H_w angles shows no considerable shift from their equilibrium values along the sampled layers. The orientation of the water molecules in the first and second monolayer is considerably influenced by the nature of the surface. The mobile crystal surface influences the water monolayer dynamics, for which orientational and bonding characteristics fluctuate rapidly. At a temperature of 300 K, this leads to a weakly bound first monolayer *vis-à-vis* the static/fixed lattice. The geometry of water molecules is similar to that reported for quantum simulations [27]. For planar surfaces, (rutile-(001) and anatase-(001)), the second monolayer is further pushed away from the surface, thereby affecting any stabilizing role played by secondary solvation of the charge transfer products/adducts created at the first ML after photo-excitation of the crystal. It can be stated that the rutile (001) and anatase (001) surfaces may play an important role by not hindering the removal of the products (H_2/O_2) formed at the first monolayer, which is a major problem with other surfaces [30]. It has been shown that these interactions between the first and second monolayers through hydrogen bonding depend on the rigidity of the first monolayer. Hopefully, these simulations will provide insights into modeling large-scale simulations or macroscopic single crystals or an ensemble of such particles in contact with water [31].

Acknowledgements

The authors acknowledge useful conversations with Dr. Damian Mooney. This material is based upon works supported by the Science Foundation Ireland (SFI) under grant No. 07/SRC/B1160, in addition to the Irish Research Council for Science, Engineering and Technology. We also thank SFI and the Irish Centre for High End Computing for the provision of high-performance computing facilities.

References

[1] U. Diebold, Surface Science Reports **48** (5–8), 53 (2003).
[2] A. Fujishima and K. Honda, Nature **238** (5358), 37 (1972).

[3] J.W. Tang, J.R. Durrant and D.R. Klug, J. Am. Chem. Soc. **130** (42), 13885 (2008).
[4] F.A. Frame and F.E. Osterloh, J. Phys. Chem. C **114** (23), 10628 (2010).
[5] K. Maeda, N. Sakamoto, T. Ikeda, H. Ohtsuka, A.K. Xiong, D.L. Lu, M. Kanehara, T. Teranishi and K. Domen, Chem.-Eur. J. **16** (26), 7750 (2010).
[6] K. Maeda, M. Higashi, D.L. Lu, R. Abe and K. Domen, J. Am. Chem. Soc. **132** (16), 5858 (2010).
[7] Y.H. Ng, A. Iwase, A. Kudo and R. Amal, J. Phys. Chem. Lett. **1** (17), 2607 (2010).
[8] M.W. Kanan and D.G. Nocera, Science **321** (5892), 1072 (2008).
[9] A. Melis and T. Happe, Plant Physiology **127** (3), 740 (2001).
[10] K. Sivula, R. Zboril, F.L. Formal, R. Robert, A. Weidenkaff, J. Tucek, J. Frydrych and M. Gratzel, J. Am. Chem. Soc. **132** (21), 7436 (2010).
[11] O. Bikondoa, C.L. Pang, R. Ithnin, C.A. Muryn, H. Onishi and G. Thornton, Nature Mater. **5** (3), 189 (2006).
[12] E. Wahlstrom, E.K. Vestergaard, R. Schaub, A. Ronnau, M. Vestergaard, E. Laegsgaard, I. Stensgaard, and F. Besenbacher, Science **303** (5657), 511 (2004); K. Onda, B. Li, J. Zhao, K.D. Jordan, J.L. Yang, and H. Petek, Science **308** (5725), 1154 (2005); R. Nakamura, T. Okamura, N. Ohashi, A. Imanishi, and Y. Nakato, J. Am. Chem. Soc. **127** (37), 12975 (2005); F. Allegretti, S. O'Brien, M. Polcik, D.I. Sayago, and D.P. Woodruff, Phys. Rev. Lett. **95** (22), 4 (2005); I.M. Brookes, C.A. Muryn, and G. Thornton, Phys. Rev. Lett. **87** (26), 4 (2001).
[13] S.J. Thompson and S.P. Lewis, Physical Review B **73** (7), 073403 (2006); M.L. Machesky, M. Predota, D.J. Wesolowski, L. Vlcek, P.T. Cummings, J. Rosenqvist, M. K. Ridley, J.D. Kubicki, A.V. Bandura, N. Kumar, and J.O. Sofo, Langmuir **24** (21), 12331 (2008); M. Machesky, M. Ridley, D. Wesolowski, D. Palmer, M. Predota, L. Vlcek, J. Kubicki, J. Sofo, A. Bandura, Z. Zhang, and P. Fenter, Geochim. Et Cosmochim. Acta **71** (15), A609 (2007); L. Vlcek, Z. Zhang, M.L. Machesky, P. Fenter, J. Rosenqvist, D.J. Wesolowski, L.M. Anovitz, M. Predota, and P.T. Cummings, Langmuir **23** (9), 4925 (2007); N. Kumar, S. Neogi, P.R.C. Kent, A.V. Bandura, J.D. Kubicki, D.J. Wesolowski, D. Cole, and J.O. Sofo, J. Phys. Chem. C **113** (31), 13732 (2009).
[14] A.V. Bandura and J.D. Kubicki, J. Phys. Chem. B **107** (40), 11072 (2003).
[15] A. Valdes, Z.W. Qu, G.J. Kroes, J. Rossmeisl and J.K. Norskov, J. Phys. Chem. C **112** (26), 9872 (2008).
[16] P. Zarzycki, J. Phys. Chem. C **111** (21), 7692 (2007).
[17] P.J.D. Lindan, N.M. Harrison and M.J. Gillan, Phys. Rev. Lett. **80** (4), 762 (1998).
[18] E. Mamontov, L. Vlcek, D.J. Wesolowski, P.T. Cummings, W. Wang, L.M. Anovitz, J. Rosenqvist, C.M. Brown and V.G. Sakai, J. Phys. Chem. C **111** (11), 4328 (2007).
[19] E. Mamontov, D.J. Wesolowski, L. Vlcek, P.T. Cummings, J. Rosenqvist, W. Wang and D.R. Cole, J. Phys. Chem. C **112** (32), 12334 (2008).
[20] M. Predota, A.V. Bandura, P.T. Cummings, J.D. Kubicki, D.J. Wesolowski, A.A. Chialvo and M.L. Machesky, J. Phys. Chem. B **108** (32), 12049 (2004).
[21] W. Langel, Surf. Sci. **496** (1–2), 141 (2002).
[22] M. Leslie W. Smith, T.R. Forester, *The DL_POLY_2 User Manual*, edited by Editor v. 2.14 ed. (2003).
[23] M. Matsui and M. Akaogi, Mol. Sim. **6**, 239 (1991).
[24] J. Goniakowski, F. Finocchi and C. Noguera, Rep. Prog. Phys. **71** (1), 016501 (2008).
[25] A. Selloni, Nature Mater. **7** (8), 613 (2008).
[26] M. Sumita, C.P. Hu and Y. Tateyama, J. Phys. Chem. C **114** (43), 18529 (2010).
[27] G. Teobaldi, W.A. Hofer, O. Bikondoa, C.L. Pang, G. Cabailh and G. Thornton, Chem. Phys. Lett. **437** (1–3), 73 (2007).
[28] J.K. Gregory, D.C. Clary, K. Liu, M.G. Brown and R.J. Saykally, Science **275** (5301), 814 (1997).
[29] X.J. Han, L. Bergqvist, P.H. Dederichs, H. Müller-Krumbhaar, J.K. Christie, S. Scandolo and P. Tangney, Phys. Rev. B **81**, 134108 (2010).
[30] L.M. Liu, P. Crawford, and P. Hu, Prog. Surf. Sci. **84** (5–6), 155 (2009); D. Pillay, Y. Wang, and G.S. Hwang, J. Am. Chem. Soc. **128** (43), 14000 (2006).
[31] A.S. Barnard, P. Zapol and L.A. Curtiss, J. Chem. Theory Comput. **1** (1), 107 (2005).